J Anim Reprod Biotechnol 2024;39:2-11
pISSN: 2671-4639 • eISSN: 2671-4663
https://doi.org/10.12750/JARB.39.1.2

JARB
Journal of Animal Reproduction and Biotechnology
Check for updates

Original Article

Establishing porcine jejunum-derived intestinal organoids to study the function of intestinal epithelium as an alternative for animal testing

Bo Ram Lee[1,*], Sun A Ock[1], Mi Ryung Park[2], Min Gook Lee[1] and Sung June Byun[3]

[1]Animal Biotechnology Division, National Institute of Animal Science, Rural Development Administration, Wanju 55365, Korea
[2]Animal Genetic Resources Research Center, National Institute of Animal Science, Rural Development Administration, Hamyang 50000, Korea
[3]Poultry Research Institute, National Institute of Animal Science, Rural Development Administration, Pyeongchang 25342, Korea

Received February 22, 2024
Revised March 12, 2024
Accepted March 12, 2024

***Correspondence**
Bo Ram Lee
E-mail: mir88@korea.kr

Author's Position and Orcid no.
Lee BR, Agriculture researcher,
https://orcid.org/0000-0002-0537-6205
Ock SA, Agriculture researcher,
https://orcid.org/0000-0002-0887-8200
Park MR, Agriculture researcher,
https://orcid.org/0000-0001-5452-5281
Lee MG, Agriculture researcher,
https://orcid.org/0000-0001-8237-6447
Byun SJ, Senior researcher,
https://orcid.org/0000-0001-6909-1025

ABSTRACT

Background: The small intestine plays a crucial role in animals in maintaining homeostasis as well as a series of physiological events such as nutrient uptake and immune function to improve productivity. Research on intestinal organoids has recently garnered interest, aiming to study various functions of the intestinal epithelium as a potential alternative to an *in vivo* system. These technologies have created new possibilities and opportunities for substituting animals for testing with an *in vitro* model.

Methods: Here, we report the establishment and characterisation of intestinal organoids derived from jejunum tissues of adult pigs. Intestinal crypts, including intestinal stem cells from the jejunum tissue of adult pigs (10 months old), were sequentially isolated and cultivated over several passages without losing their proliferation and differentiation using the scaffold-based and three-dimensional method, which indicated the recapitulating capacity.

Results: Porcine jejunum-derived intestinal organoids showed the specific expression of several genes related to intestinal stem cells and the epithelium. Furthermore, they showed high permeability when exposed to FITC-dextran 4 kDa, representing a barrier function similar to that of *in vivo* tissues. Collectively, these results demonstrate the efficient cultivation and characteristics of porcine jejunum-derived intestinal organoids.

Conclusions: In this study, using a 3D culture system, we successfully established porcine jejunum-derived intestinal organoids. They show potential for various applications, such as for nutrient absorption as an *in vitro* model of the intestinal epithelium fused with organ-on-a-chip technology to improve productivity in animal biotechnology in future studies.

Keywords: characterisation, gene expression, jejunum, intestinal organoid, porcine

INTRODUCTION

The small intestine plays a crucial role in animals in maintaining homeostasis via interacting with the microbiome and improving productivity in many physiological events, such as nutrient absorption, hormone secretion, and host-pathogen interactions from various intestinal cell types, including Paneth cells, enteroendocrine cells, goblet cells, and enterocytes (Olayanju et al., 2019; Haq et al., 2021). As a potential alternative to an *in vivo* system, intestinal organoids, have attracted much attention for studying various functions of the intestinal epithelium and creating new possibilities and opportunities for testing as an *in vitro* model instead of animal testing (Rallabandi et al., 2020; Lee et al., 2021; Park et al., 2022).

Since the first report of porcine intestinal columnar epithelial cells isolated from the neonatal piglet mid-jejunum in 1989 (Berschneider, 1989), IPEC-J2 cells have been used to investigate intestinal epithelium interactions with various pathogens, including bacteria, viruses, and fungi, and to study potential probiotic microorganisms (Brosnahan et al., 2012; Kang et al., 2023). However, IPEC-J2 cells based on *in vitro* two-dimensional (2D) culture systems face challenges in expressing the intestinal epithelium cellular diversity (Hamilton et al., 2018). Thus, scaffold-based three-dimensional (3D) culture systems have created powerful tools for cellular diversity via establishing intestinal organoids (Park et al., 2022). Concurrently, significant efforts have been made to generate intestinal organoids in various domestic animals, including chickens (Pierzchalska et al., 2017), pig (Powell and Behnke, 2017; Joo et al., 2022), cattle (Lee et al., 2021; Park et al., 2022), canine (Chandra et al., 2019), horse (Stewart et al., 2018) and goat (Kawasaki et al., 2022) and to date they are considered a focus of research.

Such technologies may provide an efficient method of generating intestinal organoids as potential alternatives to *in vivo* systems in animal biotechnology for various applications. Moreover, pigs provide an excellent model system for studying biomedicine, xenotransplantation, disease, and agricultural research because of their anatomical and physiological similarities with humans. Especially, transgenesis systems strengthen this position (Park et al., 2023). Therefore, we characterised intestinal stem cells derived from the small intestine jejunum of adult pigs and cultivated intestinal crypt-derived intestinal organoids in a 3D culture system.

In this study, we established intestinal organoids derived from the porcine jejunum to study the function of the intestinal epithelium as an alternative to using animals for testing. Furthermore, we analysed the characteristics of the intestinal organoids based on several specific markers of intestinal stem cells and the epithelium using large-scale gene expression and immunocytochemistry. We also evaluated the epithelial barrier function using an FITC-dextran 4 kDa permeability assay.

MATERIALS AND METHODS

Experimental design and animals

This study was designed with the aim of establishing porcine intestinal organoids, for the purposes of which, we used 10-month-old adult pigs, with approval granted by the Institutional Animal Care and Use Committee (IACUC) of the National Institute of Animal Science, Korea (NIAS2022-0569).

Intestinal crypt isolation and 3D cultivation

Porcine intestinal crypts from the jejunum tissue of 10-month-old adult pigs were prepared using previously described protocols (Lee et al., 2021). Briefly, the jejunum tissue was cut and opened longitudinally. The dissected fragments were washed thoroughly with washing buffer to remove the debris containing 1% penicillin/streptomycin (Sigma-Aldrich, MI, USA), after which the washed pellet was collected and resuspended in 25 mL cell disassociation solution (Stem Cell Technologies, Vancouver, Canada) and incubated at room temperature for 40 min on a rocker to release the crypts. Intestinal crypts were collected after pipetting and centrifugation at 200 × g for 5 min and resuspended in 1 mL human intestinal organoid medium (Stem Cell Technologies). Intestinal crypts were counted under an inverted microscope and resuspended in Matrigel (Corning, NY, USA) at a concentration of approximately 140-150 crypts in a 1:1 ratio to create a dome. The Matrigel dome including the intestinal crypts was then placed into the centre of a pre-warmed 24-well plate, polymerised for 15 min at 37℃, overlaid with 1 mL of human organoid medium (Stem Cell Technologies), and incubated 37℃ and 5% carbon dioxide to induce intestinal organoids.

Intestinal organoid growth, passage, and cryopreservation

Intestinal organoids were subjected to passage approximately once a week upon maturation. They experienced distinct morphological changes, such as developing spheroidal, stomatocyte, budded/elongated, and branched structures at each passage (Rozman et al., 2020). The medium was gently removed and cells were rinsed with ice-cold phosphate-buffered saline (PBS) without disturbing the organoid dome. To harvest the organoids, a 10× volume of enzyme-free cell disassociation buffer (1 mL) was added to a Matrigel dome (100 μL) in each well and incubated for 10 min. The organoids were dislodged via gentle pipetting and collected using centrifugation at 200 × g for 5 min. The pellet was resuspended in the desired quantity of medium and Matrigel at a 1:1 ratio. Each well (140-150 organoids) was distributed into three parts in sequential passages and seeded in 24-well plates. The medium was replaced every three days and sub-cultivated weekly. For cryopreservation, intestinal organoids were resuspended in preserving solution composed of 90% medium and 10% dimethyl sulfoxide (Sigma-Aldrich), stored at -80℃ for 24 h, and transferred to a liquid nitrogen tank for long-term storage.

RNA isolation

Total RNA was extracted from jejunum-derived intestinal organoids, jejunum tissue, and the muscle using TRIzol reagent (Life Technologies, CA, USA), as described previously (Lee et al., 2007; Lee et al., 2020). RNA quality was assessed via an Agilent 2100 bioanalyzer using an RNA 6000 Nano Chip (Agilent Technologies, Amstelveen, Netherlands). RNA quantification was performed using an ND 2000 Spectrophotometer (Thermo Fisher Scientific, MA, USA).

Quantitative real time polymerase chain reaction (RT-PCR)

Quantitative RT-PCR was conducted to investigate the expression of several markers of intestinal stem cells and the epithelium between jejunum-derived intestinal organoids and muscles in pigs and to validate large-scale gene expression data as described previously (Lee et al., 2023). Each total RNA sample was prepared using TRIzol reagent (Invitrogen, CA, USA). Total RNA (1 μg) was reverse transcribed using the Superscript III First-Strand Synthesis System (Invitrogen). The PCR mixture was prepared via adding 2 μL PCR buffer, 1.6 μL 2.5 mM dNTP, 10 pmol each of the forward and reverse primers, 1 μL 20× Eva green, 0.2 μL Taq DNA polymerase, and 2 μL cDNA to a final volume of 20 μL. PCR was performed in the following steps: initial incubation at 94℃ for 3 min, followed by 40 cycles at 94℃ for 30 s, 60℃ for 30 s, and 72℃ for 30 s, using a melting curve program (in-increasing temperature from 55 to 95℃ at a rate of 0.5℃ per 10 s) and continuous fluorescence measurement. Sequence-specific products were identified via generating a melting curve. Ct value represents the cycle number at which a fluorescent signal increases to significantly higher level than that of the background. Gene expression was analysed using the StepOnePlus™ Real-Time PCR System (Applied Biosystems, CA, USA) and calculated using the $2^{-\Delta\Delta}$Ct method (Livak and Schmittgen, 2001). The quantitative PCR primers used for each target gene are summarised in Table 1.

Library preparation and sequencing

Total RNA concentration was calculated, total RNA integrity was assessed, and samples were run on a TapeStation RNA screentape (Agilent Technologies). Only high-quality RNA preparations with and RNA integrity number greater than 7.0 were used for the RNA library construction. A library was independently prepared with 1 ug of

Table 1. Details of the primers used in this study for the analysis of gene expression in porcine intestinal organoids

No.	Gene name	Accession number	Forward	Reverse	Product size (bp)
1	GAPDH	NM_001206359.1	GTCGGTTGTGGATCTGACCT	AGCTTGACGAAGTGGTCGTT	210
2	LGR5	NM_001315762.1	AATTCCCTTTGCTTCCTGGT	GGGCTGATGAATGTGAGGTT	197
3	HNF4A	NM_001044571.1	AGAAATGAACCGGGTGTCTG	GCGGTCGTTGATGTAATCCT	202
4	CDH1	NM_001163060.1	CATCTTCAACCCAACCTCGT	ACGCCTTCATTGGTTACTGG	186
5	GATA6	NM_001044571.1	CTGTCCCCATGACTCCAACT	ATGTACAGCCCGTCTTGACC	178
6	MUC2	XM_021082584.1	AACTGCGAGCAATGTGTCTG	CAGGTCTGCTTGTCTGTGGA	224
7	CHGA	NM_001164005.2	TCGAGGTCATCTCTGACACG	TTCTTCTGCTGATGGGACCT	178

total RNA for each sample using Illumina TruSeq Stranded mRNA Sample Prep Kit (Illumina, Inc., CA, USA) as per manufacturer's instructions. Briefly, the poly-A containing mRNA molecules was purified using poly-T-attached magnetic beads and copied into first strand cDNA using SuperScript II reverse transcriptase (Invitrogen) and random primers. These cDNA fragments then underwent an end repair process, the addition of a single 'A' base, and adapter ligation. The products were purified and enriched using PCR to create a final cDNA library. Libraries were quantified using KAPA Library Quantification kits for Illumina Sequencing platforms according to the qPCR Quantification Protocol Guide (Kapa Biosystems, MA, USA) and qualified using a TapeStation D1000 ScreenTape (Agilent Technologies).

Data processing and analysis

Paired-end sequencing reads were generated using an Illumina NovaSeq sequencing platform. Prior to analysis, Trimmomatic v0.38 was used to remove adapter sequences and trim bases of poor quality. Cleaned reads were aligned to Sus scrofa (Sscrofa11.1) using HISAT v2.1.0 (Kim et al., 2015), based on the HISAT and Bowtie2 implementations. Reference genome sequences and gene annotation data were downloaded from the NCBI Genome Assembly and RefSeq databases, respectively. The aligned data (in SAM file format) were sorted and indexed using SAM tools v. 1.9. After alignment, transcripts were assembled and quantified using StringTie v2.1.3b (Pertea et al., 2015; Pertea et al., 2016). Gene and transcript-level quantifications were calculated as the raw read count, Fragments Per Kilobase of transcript per million mapped reads, and transcript per million mapped reads.

Differential gene expression analysis

Statistical analyses of differential gene expression were performed using edgeR v3.40.2 (Robinson et al., 2010) with raw counts as the input. In the quality control step, genes with non-zero counts in all replicates for at least one group were selected. The filtered dataset was subjected to trimmed mean of M-value normalisation to correct library size variations among samples. Statistical significance of differentially expressed genes was determined using the edgeR exactTest. Fold-changes and *p*-values were extracted from the results of the exact test. All *p*-values were adjusted using the Benjamini-Hochberg algorithm to control the false discovery rate. Significant gene list was filtered by |fold change| ≥ 2 and raw *p*-value < 0.05. Normalised values for significant genes were clustered hierarchically using these parameters (distance metric = Euclidean distance; linkage method = complete). In gProfiler, raw *p*-values were derived using a one-sided hypergeometric test and corrected to adjust the *p*-values using the Benjamini-Hochberg method. All data analyses and visualisation of differentially expressed genes were conducted using R 4.2.2 (www.r-project.org).

Immunocytochemistry

Organoids were maintained in 24-well plates until maturation. Immunocytochemistry was performed to investigate the protein expression of jejunum-derived intestinal organoids, as described previously (Lee et al., 2021). Briefly, the organoid medium and Matrigel were removed from the wells. The organoids were washed thoroughly with cold PBS and incubated in neutrally buffered 4% paraformaldehyde (Sigma-Aldrich) for 30 min at room temperature. The organoids were permeabilised in a buffer containing 0.5% Triton X-100 (Sigma-Aldrich) in PBS for 30 min at room temperature. Blocking was performed using 3% bovine serum albumin in PBS for 1 h at room temperature. The organoids were thoroughly rinsed with PBS and incubated overnight at 4℃ with requisite dilutions of the appropriate primary antibodies, as shown in Table 2. Marker protein expression was detected via incubating samples with the corresponding secondary antibodies coupled to AlexaFluor-488 and AlexaFluor-594 (Molecular Probes/Life Technologies) for 1 h at room temperature. Fluorescent samples were counterstained with diamidino-2-phenylindole (DAPI) and mounted on glass slides using ProLong Gold antifade mounting medium (Life Technologies). Images were captured using a Nikon AX confocal microscope (Nikon, Tokyo, Japan).

Table 2. Antibodies used for the functional characterization of porcine intestinal organoids

No.	Antibody	Host species	Dilution
1	LGR5	Mouse	1:100
2	Cytokeratin 19	Rabbit	1:200
3	Mucine2	Rabbit	1:200

Epithelial barrier permeability assay using FITC-dextran

Epithelial barrier function was evaluated using fluorescein isothiocyanate (FITC)-dextran (4 kDa; Sigma-Aldrich), as described previously (Lee et al., 2021). Briefly, the porcine intestinal organoids were placed in 24-well plates and allowed to grow until they fully developed into crypt and villous structures. To each well, 25 ng/mL FITC-dextran was added and the plate was incubated under normal growth conditions. Permeability was observed using luminal absorption and recorded for up to 3 h at 30-min intervals under a Nikon AX confocal microscope (Nikon). Fluorescence intensity was calculated using the ImageJ software.

Statistical analysis

Significant differences between groups were analysed via Student's *t*-test using GraphPad Prism software (version 6.0; CA, USA). The results are expressed as the mean ± standard error ($n \geq 3$, where n is the number of replicates). Differences were considered statistically significant at $p < 0.05$.

RESULTS

Growth performance and long-term maintenance of porcine jejunum-derived intestinal organoids

Intestinal crypts were isolated from the small intestine (jejunum) of healthy adult pigs (10 months old), sequentially embedded in Matrigel to form a dome, and cultured in a 3D culture system and organoid medium. Fig. 1A illustrates the growth performance timeline in 3D cultivation of porcine jejunum-derived intestinal organoids after isolating intestinal crypts. As shown in Fig. 1A, the organoids showed a spheroidal (round shaped) morphology on day 2 and mature villi and crypt-like structures on day 5 at each passage via monitoring several characteristic morphologies before passaging, indicating their recapitulating capacity, as previously described (Lee et al., 2021; Park et al., 2022). Generally, intestinal organoids under 3D culture systems toward differentiation are classified into various morphologies, such as spheroidal (round shaped), stomatocyte, budding (spheroids with extension), mature villi, and crypt-like structures during development at each passage (Rozman et al., 2020). The porcine jejunum-derived intestinal organoids grew substantially in 3D via developing spheroidal, stomatocyte, budded/elongated, and branched structures in each passage. Furthermore, they showed consistent growth on an average of 140-150 organoids per basement matrix dome from P1 to P10 in each generation, indicating continuous proliferation, long-term maintenance, and showing a high differentiation capacity for maturation on day 14 (Fig. 1B). Collectively, these results showed that porcine jejunum-derived intestinal organoids were successfully cultivated in 3D, isolated from small intestine (jejunum) crypts, and maintained long-term without losing the crypt recapitulating capacity via exhibiting several distinct morphological characteristics.

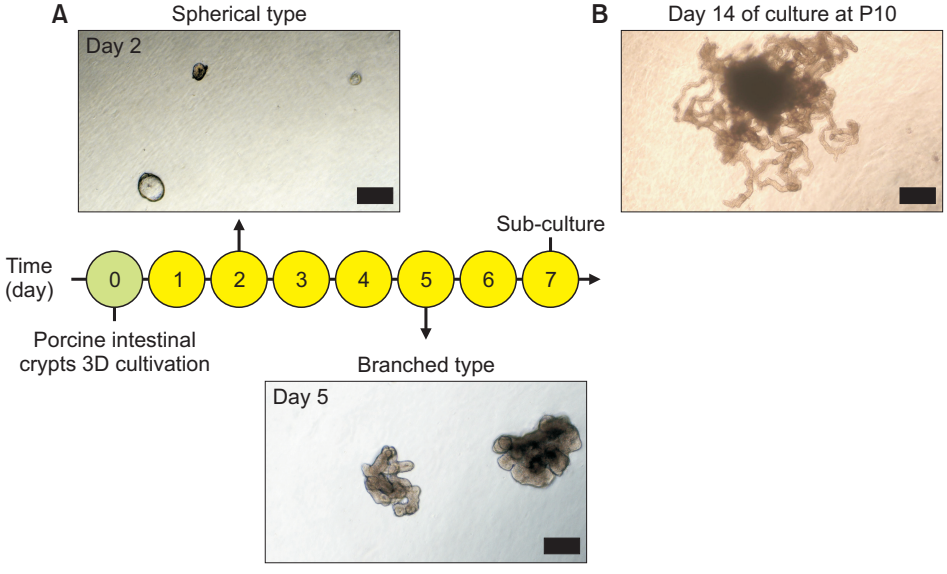

Fig. 1. Growth performance on 3D cultivation of porcine jejunum-derived intestinal organoids. (A) Porcine jejunum-derived intestinal organoids substantially grown in 3D showing spheroidal (round-shaped) morphology on day 2 and mature villi and crypt-like structures on day 5 at each passage. Spherical: 50 μm, Branched: 50 μm. (B) Porcine jejunum-derived intestinal organoids showed consistent growth on an average of 140-150 organoids per basement matrix dome from P1 to P10 at each generation, indicating continuous proliferation and long-term maintenance and showing high differentiation capacity for maturation on day 14. Scale bar: 200 μm.

Gene expression profiling of porcine jejunum-derived intestinal organoids

To investigate the genetic properties of the porcine jejunum-derived intestinal organoids for large-scale gene expression profiling, an Illumina NovaSeq sequencing platform was constructed. As shown in Fig. 2A, hierarchical clustering showed that many genes between porcine jejunum-derived intestinal organoids (J-IO-10 m) and jejunum tissue (J-10 m) in 10-month-old adult pigs were shared and similarly expressed compared to the muscle as a control. The Pearson's coefficient between J-IO-10 m and J-10 m was 0.98, indicating high similarity, whereas the Pearson's coefficient between J-IO-10 m and muscle was 0.69 (Fig. 2B), which was relatively low. Furthermore, the scatter plot revealed that specific genes related to intestinal stem cell markers such as leucine-rich

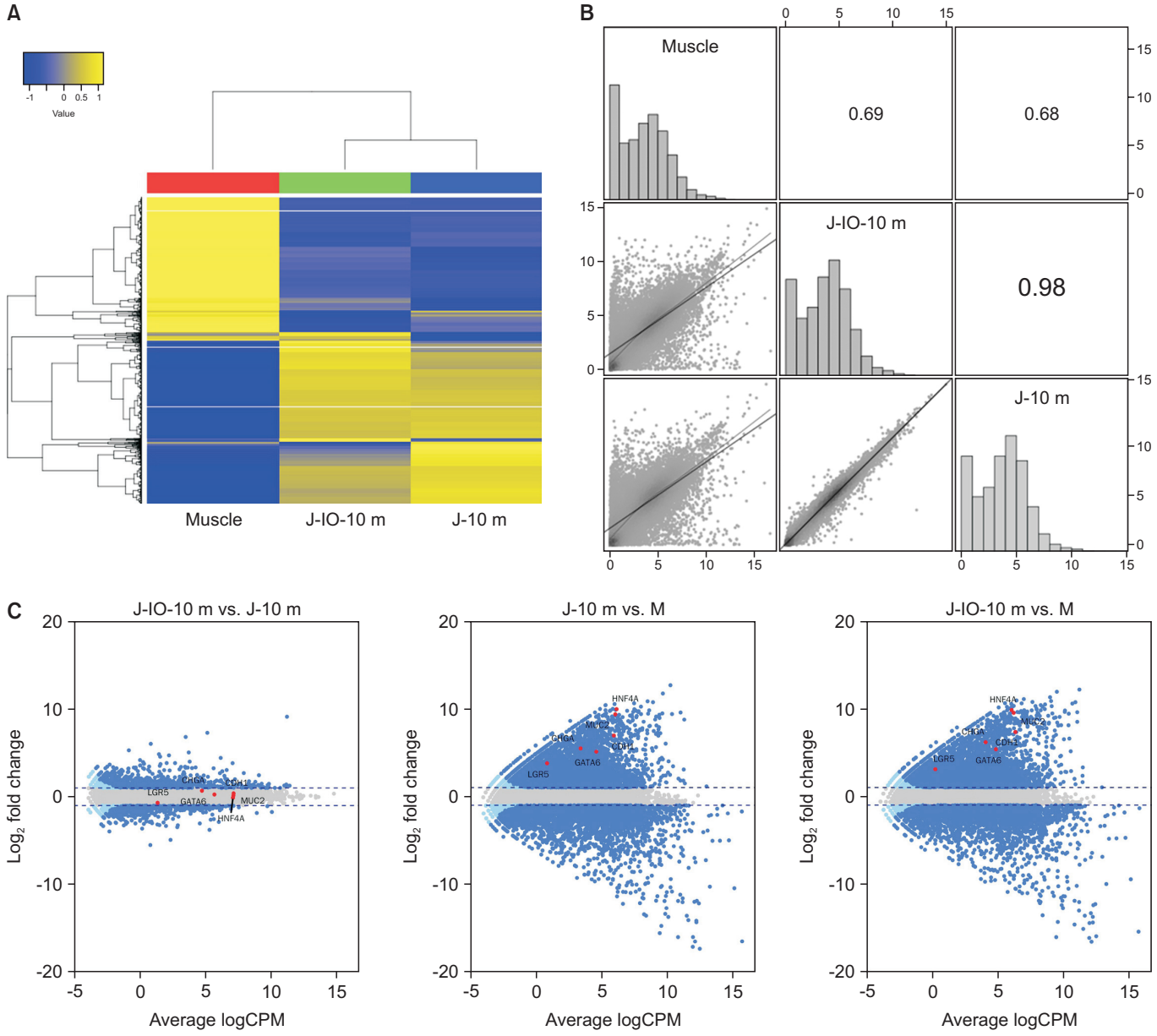

Fig. 2. Large-scale gene expression of porcine jejunum-derived intestinal organoids. (A) Hierarchical clustering showed that many genes between the porcine jejunum-derived intestinal organoids (J-IO-10 m) and jejunum tissue (J-10 m) in 10-month-old adult pigs were shared and similarly expressed compared to the muscle as a control. (B) Pearson's coefficient between J-IO-10 m and J-10 m and between J-IO-10 m and muscle (M). (C) Scatter plot revealing the upregulation of specific genes related to intestinal stem cell markers in J-IO-10 m at P5 or in J-10 m compared to M and between J-IO-10 m and J-10 m.

repeat containing G protein-coupled receptor 5 (LGR5) and hepatocyte nuclear factor 4 alpha (HNF4A), and epithelium makers such as E-cadherin (CDH1) for adherent junctions, Mucin2 (MUC2) for goblet cells, Chromogranin A (CHGA) for enteroendocrine cells, and GATA binding protein 6 (GATA6) were significantly upregulated in J-IO-10 m at P5 or in J-10 m compared to M and similar between J-IO-10 m and J-10 m (Fig. 2C). Large-scale gene expression profiling was validated and gene expression of porcine jejunum-derived intestinal organoids was further evaluated using genes involved in intestinal stem cells (LGR5 and HNF4A) and epithelium (MUC2, GATA6, CDH1, and CHGA), with muscle as a control from the prepared samples. As opposed to consisting of a single cell type, such IPEC-J2 cells, intestinal organoids comprise a diverse range of different cell types, including intestinal stem cells, Paneth cells, enterocytes, and endocrine cells (Park et al., 2022). Fig. 3 shows the quantitative RT-PCR results wherein intestinal stem cell-related genes, such as LGR5 ($p < 0.05$), HNF4A ($p < 0.001$) and those of the intestinal epithelium, such as CDH1 ($p < 0.001$), MUC2 ($p < 0.001$), CHGA ($p < 0.001$), and GATA6 ($p < 0.05$) were significantly higher on J-IO-10 m than those in the muscle. Overall, these results indicated that the genetic properties of porcine jejunum-derived intestinal organoids were highly similar to those of *in vivo* systems.

Characterisation and paracellular permeability of porcine jejunum-derived intestinal organoids

To characterise the cellular potential of porcine jejunum-derived intestinal organoids from adult pigs, we investigated the spatial expression of several specific markers involved in intestinal stem cells and epithelial characteristics at passage five. As shown in Fig. 4A, organoids showed distinct protein expression, such as that of LGR5, in intestinal stem cells. Moreover, the fluorescent-stained organoids showed epithelium-specific protein expression against Cytokeratin 19 in enterocytes and Mucin2 in goblet cells, which contributed to epithelial barrier integrity, as previously described (Lee et al., 2021), indicating that the concomitant expression of intestinal epithelial proteins in intestinal organoids derived from intestinal crypts mimicked the topology of an *in vivo* intact intestine. Furthermore, we investigated the paracellular permeability of the epithelial layer using fluorescent tracers for up to 24 h after treatment. FITC-dextran slowly entered the organoid lumen and remained constant, as shown in Fig. 4B, demonstrating high permeability for compounds of up to 4 kDa, such as glucose, peptides, and fatty acids. This indicates the presence of a mucous layer that plays a major role in nutrient absorption and barrier function. Generally, the intestinal epithelium plays key roles in the diffusion of small molecules across the intestinal barrier and the absorption of nutrients through the membrane in this barrier (Lee et al., 2021; Park et al., 2022). Together, these functional characterisations sug-

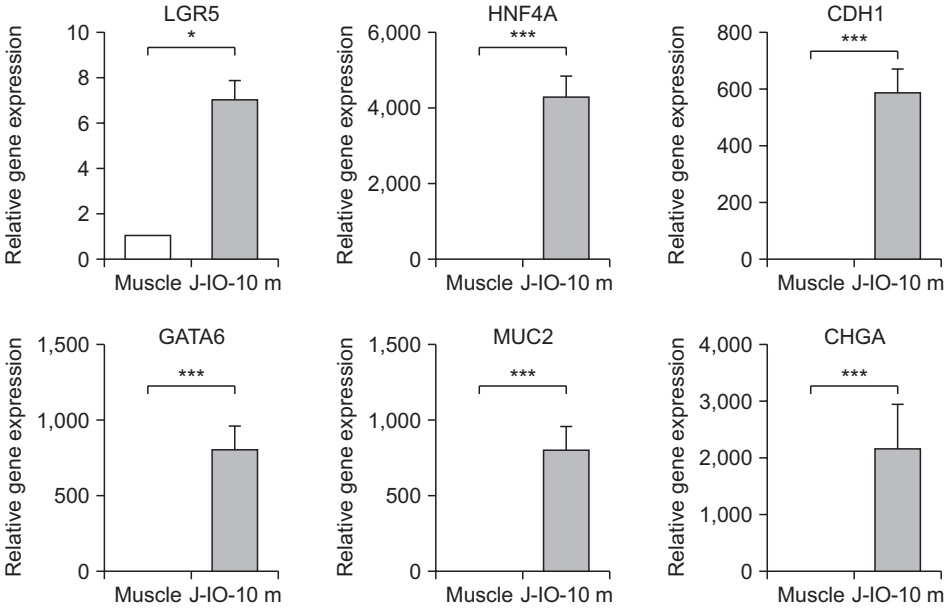

Fig. 3. Gene expression profiling of porcine jejunum-derived intestinal organoids. Quantitative real time polymerase chain reaction was performed to evaluate the gene expression of porcine jejunum-derived intestinal organoids using several markers of intestinal stem cell (LGR5 and HNF4A) and epithelial (CDH1, MUC2, CHGA, and GATA6) characteristics, with the muscle as a control from the prepared samples. Gene expression was normalised to that of GAPDH and analysed using the $2^{-\Delta\Delta}$Ct method. Significant differences between groups were analysed using Student's *t*-test. A *p*-value less than or equal to 0.05 indicated statistical significance (**p*-value ≤ 0.05, ****p*-value ≤ 0.001).

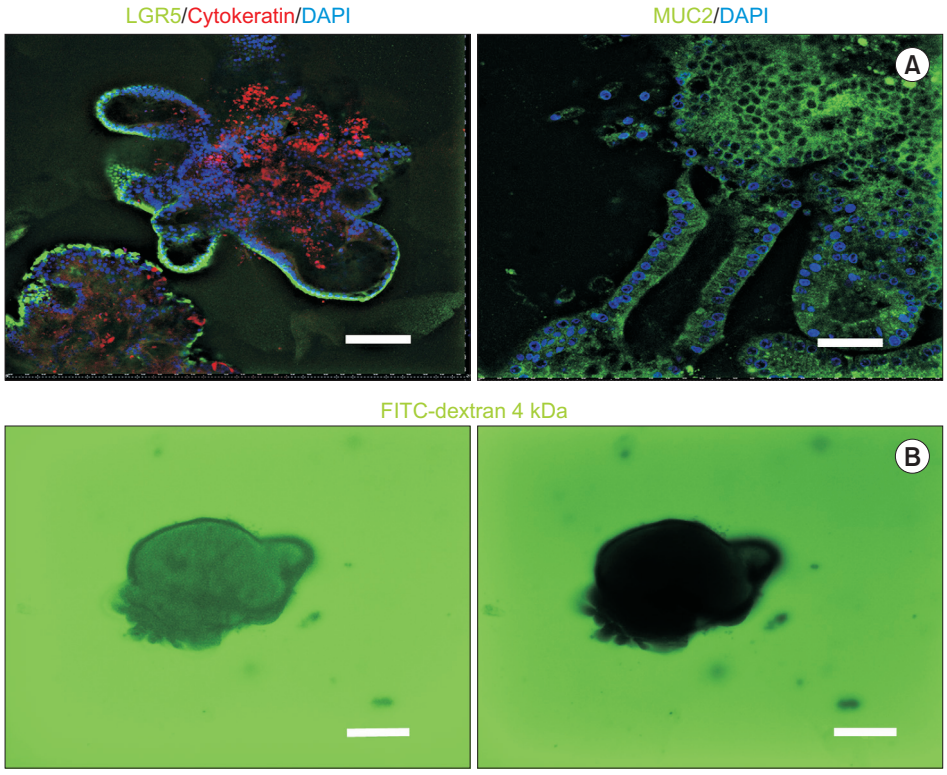

Fig. 4. Characterisation and paracellular permeability of porcine jejunum-derived intestinal organoids. (A) Immunostaining of LGR5, Cytokeratin 19, and Mucin2 in porcine jejunum-derived intestinal organoids at passage 5. Organoids were counterstained with DAPI. Scale bar: 100 μm. (B) Paracellular permeability of the epithelial layer in porcine jejunum-derived intestinal organoids using fluorescent tracers. Scale bar: 100 μm.

gest that porcine jejunum-derived intestinal organoids are physiologically relevant to the *in vivo* gut absorption properties.

DISCUSSION

The findings of recent studies have highlighted the considerable potential of intestinal organoids as *in vitro* models that can be used as an alternative to animals for various test procedures (Rallabandi et al., 2020; Lee et al., 2021; Park et al., 2022). In the present study, using a 3D culture system, we successfully established porcine jejunum-derived intestinal organoids.

Initially, we used isolated intestinal crypts, including intestinal stem cells, derived from the jejunum of the small intestines of healthy adult pigs (10 months old), which were embedded within a Matrigel dome. The organoids thus obtained, which were maintained over the long term and cultivated using a scaffold-based method, were found to have several distinct morphological characteristics, including spheroidal, stomatocyte, budded/elongated, and branched structures, during each successive passage, as shown in Fig. 1A. Furthermore, we confirmed the stable growth performance during several passages (> P10), as well as the differentiation capacity of these organoids (Fig. 1B). Our findings in this study are consistent with those reported previously with respect to bovine intestinal organoids (Lee et al., 2021), thereby indicating that porcine jejunum-derived intestinal organoids derived from jejunum crypts of the small intestine can be maintained over the long term without loss of the recapitulating capacity of crypts, and also closely mimic the *in vivo* organ physiology.

With regards to the genetic properties of porcine jejunum-derived intestinal organoids determined based on large-scale gene expression profiling and quantitative RT-PCR, when compared with muscle, we detected a high similarity between intestinal organoids and the small intestine (Fig. 2). Moreover, our detection of cellular diversity indicative of the intestinal epithelium comprising a range of different cell types, including intestinal stem cells, Paneth cells, enterocytes, and endocrine cells (Fig. 3), provides evidence of the physiological similarity between the intestinal organoids and small intestine at the gene expression level. Furthermore, we also investigated the spatial expression of specific markers associated with intestinal stem cells, and using fluorescent tracers, examined the characteristics and paracellular permeability of the epithelial layer. As shown in Fig. 4A, the porcine

jejunum-derived intestinal organoids were found to be characterised by distinct expression patterns, such as that of LGR5 associated with self-renewal capacities, and also showed epithelium-specific expression of Cytokeratin 19 and Mucin2 associated with enterocytes and goblet cells, respectively, thereby providing evidence to indicate the presence of mucin-secreting goblet cells. On the basis of these findings, it would thus appear that the porcine jejunum-derived intestinal organoids have a cellular profile resembling that of the *in vivo* porcine small intestine, and that in this regard, these organoids are similar to previously developed bovine intestinal organoids (Lee et al., 2021; Park et al., 2022).

In vivo, the primary roles of the epithelial barrier are paracellular permeability and nutrient absorption (Rallabandi et al., 2020), and accordingly, in the present study, we evaluated these functions in the intestinal organoids *in vitro* based on an FITC-dextran 4 kDa uptake assay. Our observations revealed the slow and constant entry of FITC-dextran into the organoid lumen, thereby tending to indicate the presence of a mucous layer that plays a major role in nutrient absorption and barrier function (Fig. 4B). On the basis of these findings, we thus speculate that the porcine jejunum-derived intestinal organoids developed in the study could have potential application as an *in vitro* model for the absorption of nutrients such as glucose, peptides, and fatty acids.

CONCLUSION

In this study, we successfully established porcine jejunum-derived intestinal organoids using a 3D culture system. They have potential for various applications; for example, they may be used in comparative assessments of nutrient absorption efficiency and the development of feed additives as an *in vitro* model of the intestinal epithelium fused with organ-on-a-chip technology to improve productivity in animal biotechnology.

Author Contributions: Conceptualization, B.R.L.; methodology, data curation and formal analysis, B.R.L., S.A.O., M.R.P., M.G.L., S.J.B.; writing-original draft preparation, B.R.L.; supervision, B.R.L.; funding acquisition and project Administration, B.R.L. All authors have read and agreed to the published the final version of the manuscript.

Funding: This work was carried out with the support of "Cooperative Research Program for Agriculture Science and Technology Development (Project No. PJ01671901)" Rural Development Administration (RDA), Republic of Korea.

Ethical Approval: The experimental use of adult pig was approved by the Institutional Animal Care and Use Committee (IACUC) of the National Institute of Animal Science (NIAS2022-0569), Korea.

Consent to Participate: Not applicable.

Consent to Publish: Not applicable.

Availability of Data and Materials: Not applicable.

Acknowledgements: None.

Conflicts of Interest: No potential conflict of interest relevant to this article was reported.

REFERENCES

Berschneider HM. 1989. Development of normal cultured small intestinal epithelial cell lines which transport Na and Cl. Gastroenterology 96(Suppl Pt 2):A41.

Brosnahan AJ and Brown DR. 2012. Porcine IPEC-J2 intestinal epithelial cells in microbiological investigations. Vet. Microbiol. 156:229-237.

Chandra L, Borcherding DC, Kingsbury D, Atherly T, Ambrosini YM, Bourgois-Mochel A, Yuan W, Kimber M, Qi Y, Wang Q, Wannemuehler M, Ellinwood NM, Snella E, Martin M, Skala M, Meyerholz D, Estes M, Fernandez-Zapico ME, Jergens AE, Mochel JP, Allenspach K. 2019. Derivation of adult canine intestinal organoids for translational research in gastroenterology. BMC Biol. 17:33.

Hamilton CA, Young R, Jayaraman S, Sehgal A, Paxton E, Thomson S, Katzer F, Hope J, Innes E, Morrison LJ, Mabbott NA. 2018. Development of *in vitro* enteroids derived from bovine small intestinal crypts. Vet. Res. 49:54.

Haq I, Yang H, Ock SA, Wi HY, Park KW, Lee PY, Choi HW, Lee BR. 2021. Recent progress and future perspectives on intestinal organoids in livestock. J. Agric. Life Sci. 55:83-90.

Joo SS, Gu BH, Park YJ, Rim CY, Kim MJ, Kim SH, Cho JH, Kim HB, Kim M. 2022. Porcine intestinal apical-out organoid model for gut function study. Animals (Basel) 12:372.

Kang TH, Shin S, Park J, Lee BR, Lee SI. 2023. Pyroptosis-mediated damage mechanism by deoxynivalenol in porcine small intestinal epithelial cells. Toxins (Basel) 15:300.

Kawasaki M, Goyama T, Tachibana Y, Nagao I, Ambrosini YM. 2022. Farm and companion animal organoid models in translational research: a powerful tool to bridge the gap between mice and humans. Front. Med. Technol. 4:895379.

Kim D, Langmead B, Salzberg SL. 2015. HISAT: a fast spliced aligner with low memory requirements. Nat. Methods 12:357-360.

Lee BR, Kim H, Park TS, Moon S, Cho S, Park T, Lim JM, Han JY. 2007. A set of stage-specific gene transcripts identified in EK stage X and HH stage 3 chick embryos. BMC Dev. Biol. 7:60.

Lee BR, Rengaraj D, Choi HJ, Han JY. 2020. A novel F-box domain containing cyclin F like gene is required for maintaining the genome stability and survival of chicken primordial germ cells. FASEB J. 34:1001-1017.

Lee BR and Yang H. 2023. *In vitro* culture of chicken embryonic stem cell-like cells. J. Anim. Reprod. Biotechnol. 38:26-31.

Lee BR, Yang H, Lee SI, Haq I, Ock SA, Wi H, Lee HC, Lee P, Yoo JG. 2021. Robust three-dimensional (3D) expansion of bovine intestinal organoids: an *in vitro* model as a potential alternative to an *in vivo* system. Animals (Basel) 11:2115.

Livak KJ and Schmittgen TD. 2001. Analysis of relative gene expression data using real-time quantitative PCR and the 2(-Delta Delta C(T)) method. Methods 25:402-408.

Olayanju A, Jones L, Greco K, Goldring CE, Ansari T. 2019. Application of porcine gastrointestinal organoid units as a potential *in vitro* tool for drug discovery and development. J. Appl. Toxicol. 39:4-15.

Park KW, Yang H, Lee MG, Ock SA, Wi H, Lee P, Hwang IS, Yoo JG, Park CK, Lee BR. 2022. Establishment of intestinal organoids from small intestine of growing cattle (12 months old). J. Anim. Sci. Technol. 64:1105-1116.

Park KW, Yang H, Wi H, Ock SA, Lee P, Hwang IS, Lee BR. 2022. Effect of Wnt signaling pathway activation on the efficient generation of bovine intestinal organoids. J. Anim. Reprod. Biotechnol. 37:136-143.

Park MR, Ahn JS, Lee MG, Lee BR, Ock SA, Byun SJ, Hwang IS. 2023. Characterization of enlarged tongues in cloned piglets. Curr. Issues Mol. Biol. 45:9103-9116.

Pertea M, Kim D, Pertea GM, Leek JT, Salzberg SL. 2016. Transcript-level expression analysis of RNA-seq experiments with HISAT, StringTie and Ballgown. Nat. Protoc. 11:1650-1667.

Pertea M, Pertea GM, Antonescu CM, Chang TC, Mendell JT, Salzberg SL. 2015. StringTie enables improved reconstruction of a transcriptome from RNA-seq reads. Nat. Biotechnol. 33:290-295.

Pierzchalska M, Panek M, Czyrnek M, Gielicz A, Mickowska B, Grabacka M. 2017. Probiotic Lactobacillus acidophilus bacteria or synthetic TLR2 agonist boost the growth of chicken embryo intestinal organoids in cultures comprising epithelial cells and myofibroblasts. Comp. Immunol. Microbiol. Infect. Dis. 53:7-18.

Powell RH and Behnke MS. 2017. WRN conditioned media is sufficient for *in vitro* propagation of intestinal organoids from large farm and small companion animals. Biol. Open 6:698-705.

Rallabandi HR, Yang H, Oh KB, Lee HC, Byun SJ, Lee BR. 2020. Evaluation of intestinal epithelial barrier function in inflammatory bowel diseases using murine intestinal organoids. Tissue Eng. Regen. Med. 17:641-650.

Robinson MD, McCarthy DJ, Smyth GK. 2010. edgeR: a Bioconductor package for differential expression analysis of digital gene expression data. Bioinformatics 26:139-140.

Rozman J, Krajnc M, Ziherl P. 2020. Collective cell mechanics of epithelial shells with organoid-like morphologies. Nat. Commun. 11:3805.

Stewart AS, Freund JM, Gonzalez LM. 2018. Advanced three-dimensional culture of equine intestinal epithelial stem cells. Equine Vet. J. 50:241-248.